Comparative evaluation of radioiodine-labeled 1-(2′-fluoro-2-deoxy-D-arabinofuranosyl)-5-iodouracil (FIAU) and 1-(2′-fluoro-2-deoxy-D-ribofuranosyl)-5-iodouracil (FIRU) for molecular imaging

Su Hee Hong

The Graduate School
Yonsei University
Department of Biomedical Laboratory Science

Comparative evaluation of radioiodine-labeled 1-(2′-fluoro-2-deoxy-D-arabinofuranosyl)-5-iodouracil (FIAU) and 1-(2′-fluoro-2-deoxy-D-ribofuranosyl)-5-iodouracil (FIRU) for molecular imaging

A Master's Thesis submitted to the Department of Biomedical Laboratory Science and the Graduate School of Yonsei University in partial fulfillment of the requirements for the degree of Master of Science in Biomedical Laboratory Science

Su Hee Hong

June, 2008

This certifies that the master's thesis of Su Hee Hong is approved.

_____

Thesis Supervisor: Yong Serk Park

_____

Jong Bae Kim: Thesis Committee Member

_____

Ok Doo Awh: Thesis Committee Member

The Graduate School

Yonsei University

June, 2008

CONTENTS

LIST OF FIGURES ····· Ⅵ

LIST OF TABLES ····· Ⅷ

ABBREVIATIONS ····· Ⅸ

ABSTRACT ····· X

Ⅰ. INTRODUCTION ····· 1

Ⅱ. MATERIALS AND METHODS ····· 8

1. Materials ····· 8
2. Preparation of radiolabeled nucleoside analogues ····· 9
3. Cell line and culture ····· 12
4. Assays for cytotoxcicity and cell proliferation ····· 12
5. Cellular uptakes of radioactive iodine-labeled FIAU and FIRU · 13
6. Subcutaneously and intravenously xenografted nude mice as a tumor model ····· 14
7. Imaging of tumor-xenografted mice with a microPET and a γ-camera ····· 15
8. Image analysis ····· 16

Ⅲ. RESULTS

1. Radiolabeling of FIAU and FIRU ····· 17
2. Cytotoxicities of non-radiolabeled nucleoside analogues ····· 19
3. Cellular uptakes of [^{125}I]FIAU and [^{125}I]FIRU ····· 22
4. γ-camera images of MCA and MCA-TK tumors in mice ····· 24
5. MicroPET images of MCA and MCA-TK tumors in mice ····· 26
6. Analysis of the microPET images ····· 28
7. Imaging of *in vivo* tumor cell trafficking and metastasized

tumors ·····30
Ⅳ. DISCUSSION ·····32
Ⅴ. REFERENCES ·····36
국문 요약 ·····44
감사의 글 ·····46

LIST OF FIGURES

Figure 1. Reporter gene expression and trapping of nucleoside analogues in cells ·····4

Figure 2. The chemical structures of HSV1-TK enzyme substrates ·····5

Figrue 3. The radio-labeling and chemical structure of [^{124,125,131}I]FIAU and [^{124,125,131}I]FIRU ·····11

Figure 4. Reverse phase chromatography elution profile of [^{124,125,131}I]FIAU and [^{124,125,131}I]FIRU ·····18

Figure 5. Cytotoxicity of FIAU, FIRU, GCV and DMSO in MCA and MCA-TK cells ·····20

Figure 6. Cellular uptakes of [^{125}I]FIAU and [^{125}I]FIRU by MCA and MCA-TK cells ·····23

Figure 7. Planar γ-camera images of mice carrying MCA-TK or MCA tumors after injection of [^{124}I]FIAU and [^{124}I]FIRU ·····25

Figure 8. Representative serial microPET images of mice carrying MCA-TK or MCA tumors after injection of [^{124}I]FIAU and [^{124}I]FIRU ·····27

Figure 9. Serial γ-camera imaging of MCA and MCA-TK cell trafficking and metastasized tumors ·····31

LIST OF TABLES

Table 1. The characteristics of radioiodine ·····6

Table 2. The characteristics of imaging modalities ·····7

Table 3. HPLC conditions for preparation of [^{124,125,131}I]FIAU and [^{124,125,131}I]FIRU ·····10

Table 4. IC_{50} of nucleoside analogues of FIAU, FIRU, GCV and DMSO in MCA and MCA-TK cells ·····21

Table 5. The %ID/g of [^{124}I]FIAU and [^{124}I]FIRU in mice bearing MCA-TK or MCA tumors ·····29

ABBREVIATIONS

FIAU: 1-(2′-fluoro-2-deoxy-D-arabinofuranosyl)-5-iodouracil

FIRU: 1-(2′-fluoro-2-deoxy-D-ribofuranosyl)-5-iodouracil

[*I]FIAU: (1-(2′-fluoro-2-deoxy-D-arabinofuranosyl)-5-[*I]iodouracil)

[*I]FIRU: (1-(2′-fluoro-2-deoxy-D-ribofuranosyl)-5-[*I]iodouracil)

GCV: ganciclovir

HPLC: high performance liquid chromatography

HSV1-TK: herpes simplex virus type 1 thymidine kinase

MCA : MCA-RH7777 cell

MCA-TK : HSV1-TK gene drived MCA cell

MTS: 3-[4,5-dimethylthiazol-2-yl]-5-(3-carboxymethoxyphenyl)
-2-(4-sulfophenyl)-2H-tetraxolium

PET: positron emission tomography

ROI: region of interest

%ID: percentage of injected dose

%ID/g: percentage of injected dose per gram

γ-camera: gamma-camera

Comparative evaluation of radioiodine-labeled 1-(2′-fluoro-2-deoxy-D-arabinofuranosyl)-5-iodouracil (FIAU) and 1-(2′-fluoro-2-deoxy-D-ribofuranosyl)-5-iodouracil (FIRU) for molecular imaging

ABSTRACT

The goal of this investigation is to evaluate the efficiencies of the FIAU (1-(2′-fluoro-2-deoxy-D-arabinofuranosyl)-5-iodouracil) and FIRU (1-(2′-fluoro-2-deoxy-D-ribofuranosyl)-5-iodouracil) as a potential tracer for reporter gene imaging with microPET and γ-camera imaging of herpes simplex virus type 1 thymidine kinase (HSV1-TK)-expressing cells xenografted in mice. [*I]FIAU and [*I]FIRU have 2′-arabinofluoro and 2′-ribofluoro substitution, respectively. To examine the characteristics of two different configurations of FIAU and FIRU, a series of biological evaluations were performed in HSV1-TK gene-expressing cells and mice with HSV1-TK gene-expressing tumor

xenograft.

FIAU and FIRU were radiolabeled with [^{124}I], [^{125}I] and [^{131}I] using a H_2O_2 oxidizing agent and purified by high performance liquid chromatography (HPLC). Their radiochemical purity was <99% by HPLC. For cytotoxicity analysis of FIAU and FIRU, MCA rat hepatoma cells and MCA-TK (HSV1-TK-positive) cells were treated with FIAU, FIRU, or GCV (ganciclovir) and their viabilities were measured by the MTS method 5 days later. FIAU was more toxic than GCV in MCA and MCA-TK cells while FIRU was less toxic to the both cell lines. Cellular uptakes of [^{125}I]FIAU and [^{125}I]FIRU were analysed at 0.5 h, 1 h, 2 h, and 4 h post treatment. The uptakes of [^{125}I]FIAU and [^{125}I]FIRU by MCA-TK cells were 30.2 and 15.0 %ID, respectively. The uptakes by MCA-TK cells were higher than those by MCA cells. [^{124,131}I]FIAU and [^{124,131}I]FIRU were administered to mice bearing MCA or MCA-TK cells. Molecular images of the treated mice were obtained with a microPET and γ-camera at various time-points. [^{124}I]FIAU and [^{124}I]FIRU exhibited 7.11 and 0.15 %ID/g in the ROIs (regions of interest) of tumor region, respectively. In the microPET image analysis, [^{124}I]FIAU showed higher %ID/g values than [^{124}I]FIRU in the both tumor mouse models. Imaging of tumor cell trafficking in mice carrying metastasized MCA-TK tumors was obtained with γ-camera at several time points. However, metastasized regions of the tumors were not localized.

The experimental results in this thesis suggest that the radiolabeled FIAU can be utilized as an efficient imaging agent for long term trafficking of HSV1-TK-expressing cells, such as varied types of stem cells and immune cells.

Key words : Reporter gene, HSV1-TK, FIAU, FIRU, PET, γ-camera

Ⅰ. INTRODUCTION

The reporter gene concept has become a standard in various molecular biology protocols [1-6]. In general, the function of the promoter and other regulatory regions of a gene are assessed through the regulated expression of a reporter gene. Imaging of transgene expression is largely independent of the vector used to shuttle the reporter gene into the cells of the target tissue, where any of several currently available vectors can be used (eg, retrovirus, adenovirus, adeno-associated virus, lentivirus, liposomes, etc.) [3]. Reporter genes include cytosine deaminase (CD), green fluorescence protein (GFP), luciferase (LUC) and herpes simplex virus type 1 thymidine kinase (HSV1-TK) [1-8].

Varied reporter genes encoding reporter proteins that can be efficiently detected in a living animal through injection of specific substrates has been developed for a number of different experimental purposes (Figure 1). Methods for repeated, non-invasive, and quantitative images of gene expression in living animals are rapidly emerging and change studies of gene expression *in vivo* [3, 9]. Noninvasive imaging of transgene expression would be of considerable value in many ongoing and future clinical gene therapy trials by defining the location, magnitude, and persistence of transgene expression over time [10-11].

Recently, HSV1-TK is the most widely used "reporter genes" for radiotracer-based molecular imaging using microPET (micro positron emission tomography), SPECT (single photon emission computed tomograpy), and γ-camera. It has been also utilized as a "suicide gene" for gene therapy of cancer. Small-animal microPET imaging of *in vivo* expression of HSV1-TK using corresponding reporter probes provides valuable information for monitoring gene therapy of cancers [6, 12-16].

The mammalian thymidine kinase (TK) is a key enzyme in the *de novo*

pathway of DNA synthesis. This rate limiting enzyme catalyzes the monophosphosphorylation of thymidine to dTMP. The monophosphate dTMP is subsequently converted to diphosphate dTDP and then triphosphate dTTP. Ultimately, dTTP becomes a substrate useful only for DNA synthesis but not for RNA synthesis [17]. Also, HSV-TK enzyme for the first two steps of phosphorylation is more activated with non-natural nucleoside analogues, and cellular kinase is activated for the final step [18-20].

In contrast to the mammalian TK enzyme, which phosphorylates thymidine preferentially, HSV1-TK has a substantially broad specificity. For this reason, it has been possible to develop highly effective, but less toxic anti-herpes virus agents such as acyclovir (ACV) and ganciclovir (GCV). Also, 2′-fluoro-2′-deoxyuridine derivatives are primarily phosphorylated only by the HSV1-TK enzyme. This difference in substrate specificity has made HSV1-TK an excellent choice for cancer gene therapy, both as cytotoxicity and as reporter mechanism [6, 12, 15, 21, 22].

Tjuvajev et al., assessed whether animal imaging with radiolabeled FIAU (1-(2′-fluoro-2-deoxy-D-arabinofuranosyl)-5-iodouracil) [10, 23, 24] was sufficiently sensitive to monitor HSV1-TK gene expression after *in vivo* retroviral transduction to s.c. pre-established RG2 (rat glioma cell) and W256 (mammary carcinoma cell) tumors. FIRU was accumulated highly selectively in tumors expressing the HSV1-TK genes [25].

Several nucleosides, ribosyl or acyclic nucleosides having a radiolabeled pyrimidine or purine (Figure 2), have been reported as a potent imaging agent to detect the expression of HSV1-TK gene [10, 12, 17, 21, 26-29].

In a number of researches, compounds with fluorine in the 2′ and 3′ positions of deoxyribose have been studied as therapeutic and imaging agents. Additional modifications within the sugar ring have been introduced to synthesize varied nucleoside analogues such as FIAU and FIRU [30, 31]. FIAU

has a 2′-fluoro substituent in the arabino configuration while FIRU has a 2′-fluoro substituent in the ribo configuration. According to previous studies, FIAU and FIRU were more desirable substrates for the HSV1-TK enzymes [10, 17, 21, 27-29].

Imaging probes such as radiolabeled nucleoside analogues can be used to assess vector targeting, to evaluate the level of suicide gene (HSV1-TK) expression, and to quantitatively monitor the level of the therapeutic enzyme during gene therapy [26, 32]. [^{124}I] is a radioisotope that can be visualized in PET because of the positron release from the radio-iodine nucleus. [^{131}I] has been used in nuclear medicine as an imaging isotope for γ-camera and a radiotherapeutic agent. Other radioisotopes are also used in nuclear medicine (Table 1). Nuclear medicine techniques, such as PET and γ-camera, can provide repeated, non-invasive and quantitative assessments of the expression of genes in tissues and organs. In animal models, imaging of HSV1-TK transduced malignant tumors was successfully acquired by microPET and γ-camera [13, 33-37]. MicroPET and γ-camera are sensitive modalities to obtain quantitative imaging data. Also, they required only nanogram amount of probe, which is nontoxic. Characteristics of microPET and γ-camera are summarized in Table 2 [38, 39].

In this study, FIAU and FIRU were evaluated their effectiveness as a potential tracer for imaging of HSV1-TK expression with microPET and γ-camera. Also, the biological *in vitro* and *in vivo* characteristics of FIAU and FIRU, which have a different configuration at 2′ position, were examined and compared to each other.

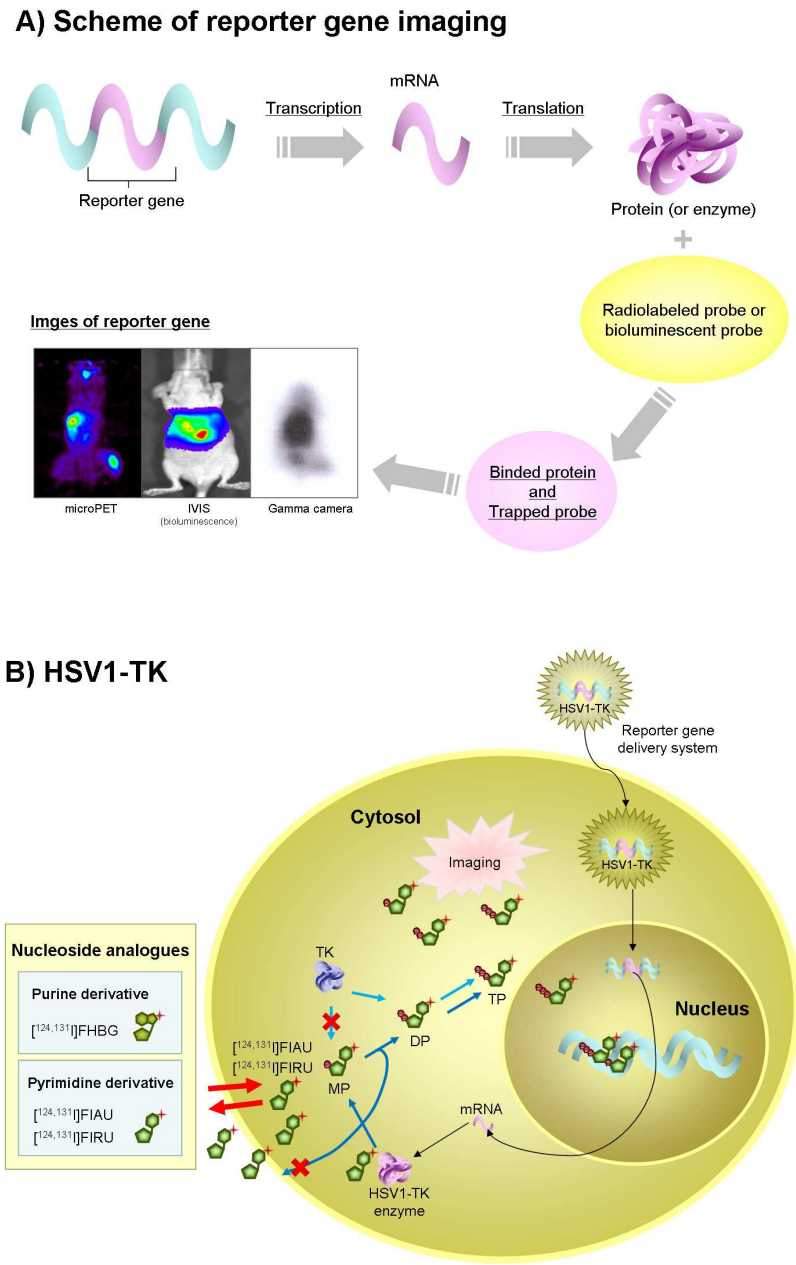

Figure 1. Reporter gene expression and trapping of nucleoside analogues in cells. Herpes simplex virus type 1 thymidine kinase, HSV1-TK; thymidine kinase, TK; thymonophosphate, MP; diphosphate, DP; triphosphate, TP.

Pyrimidine derivative

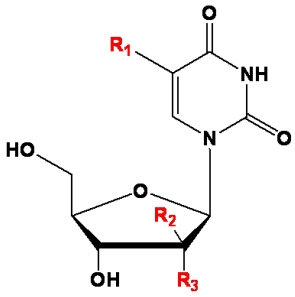

Compounds	R_1	R_2	R_3
FIAU	I	F	H
FIRU	I	H	F
FMAU	CH_3	F	H
IVFRU	CH_2=CH_2-I	H	F
IUdR	I	H	H
BrUdR	Br	H	H

Purine derivative

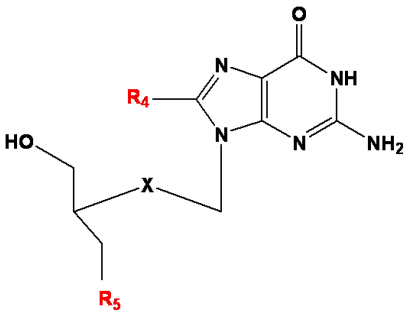

Compounds	X	R_4	R_5
GCV	O	OH	H
PCV	CH_2	OH	H
FGCV	O	OH	F
FPCV	CH_2	OH	F
FHPG	O	F	H
FHBG	CH_2	F	H

Figure 2. The chemical structures of HSV1-TK enzyme substrates (Acad Radiol, 2005; 12:798-805)

Table 1. The characteristics of radioiodine

Radio isotope	Half-life time	Energy (KeV)	Decay mode	Application
^{123}I	13.2 days	159.10	γ	γ-camera
^{124}I	4.18 days	511	β, γ	PET
^{125}I	60.14 days	35.46	Electrons	*In vitro*
^{131}I	8.04 days	364.48	γ, β	γ-camera

Table 2. The characteristics of imaging modalities

Technique	Resolution *	Depth	Time †	Quantitative ‡	Multi-channel	Imaging agents	Target	Cost §	Main small-animal use	Clinical use
MRI	10-100 μm	No limit	Minutes to hours	Yes	No	Paramagnetic chelates, magnetic particles	Anatomical, physiological, molecular	$$$	Versatile imaging modality with high soft-tissue contrast	Yes
CT	50 μm	No limit	Minutes	Yes	No	Iodinated molecules	Anatomical, physiological	$$	Imaging lungs and bone	Yes
PET	1-2 mm	No limit	Minutes to hours	Yes	No	^{18}F, ^{124}I, ^{64}Cu- or ^{11}C-labeled compounds	Physiological, molecular	$$$	Versatile imaging modality with many tracers	Yes
SPECT (γ-camera)	1-2 mm	No limit	Minutes to hours	Yes	No	^{131}I, ^{99m}Tc- or ^{111}In-labeled compounds	Physiological, molecular	$$	Imaging labeled antibodies, proteins and peptides	Yes
Fluorescence reflectance imaging	2-3 mm	<1 cm	Seconds to minutes	No	Yes	Photoproteins, fluorochromes	Physiological, molecular	$	Rapid screening of molecular events in surface-based disease	Yes
Bioluminescence imaging	Several mm	Cm	Minutes	No	Yes	Luciferins	molecular	$$	Gene expression, cell and bacterium tracking	No

*For high-resolution, small-animal imaging systems.
†Time for image acquisition.
‡Quantitative here means inherently quantitative. All approaches allow relative quantification.
§Cost is based on purchase price of imaging systems in the United States: $, <US$100,000; $$, US$100,000–300,000; $$$, >US$300,000.
From Nature, 2008; 452:580-589.

Ⅱ. MATERIALS AND METHODS

1. Materials

Carrier-free sodium [^{125,131}I]iodide were purchased from Korea Atomic Energy Research Institute (KAERI, Daejeon, Korea) and carrier-free sodium [^{124}I]iodide was produced by using 50 MeV cyclotron in Korea Institute of Radiological and Medical Sciences (KIRAMS, Seoul, Korea). FIAU was purchased from Future Chem (Seoul, Korea) and FIRU was kindly provided from the Laboratory of Radiopharmaceuticals, KIRAMS. The MCA-RH7777 (MCA, CRL1601) rat hepatoma cell line was purchased from ATCC. Thymdine kinase (TK)-transduced MCA cells (MCA-TK) [40] were kindly provided from Dr. Kwon of Molecular Oncology Laboratory, KIRAMS. 3-[4,5-dimethylthiazol-2-yl]-5-(3-carboxymethoxyphenyl)-2-(4-sulfophenyl)-2H-tetraxolium, inner salt (MTS) was purchased from Promega (Madison, USA).

2. Preparation of radiolabeled nucleoside analogues

Radioiodinated FIAU and FIRU were prepared by iododestannylation using carrier-free sodium [^{124,125,131}I]iodide and 30% H_2O_2 (Sigma, St. Louis, USA) oxidizing agent. Carrier-free sodium [^{124,125,131}I]iodide in 0.01 N NaOH was added into a reaction vial containing 0.1-0.5 ml of distilled water. FIAU or FIRU (each 100 μg) in ethyl alcohol (Sigma, St. Louis, USA) were added to the vial. Two μL of 1 N HCl (Sigma, St. Louis, USA) was added in order to reach pH 4-5. Fifty μL of 30% H_2O_2 was added to the reaction mixture, which was then incubated for 30 min at room temperature.

The resulting radioiodinated FIAU and FIRU were purified by reverse phase high-performance liquid chromatography (HPLC; Younglin, Seoul, Korea) with C-18 column (3.9×300 mm, Waters, Milford, USA) using gradient elution with distilled water and ethanol (Sigma, St. Louis, USA) [41]. The elution conditions of HPLC is shown in Table 3. The concentration of ethanol containing 0.1% trifluoroacetic acid (Sigma, St. Louis, USA) was increased from 5% to 80% over a period of 20 min at a flow rate of 2 mL/min: 5% ethanol elution for 1-5 min, 80% ethanol gradient elution for 5-20 min, and 5% ethanol isocratic elution for 20-35 min. The retention time of radiolabeled compounds were determined using a UV and radioactivity detector (Raytest, Straubenhardt, Germany) [41]. The radiochemical purity was determined by thin layer chromatography (solvent; dichloromethane/methyl alcohol, 9/1). The solvent was evaporated under a stream of argon gas and the [^{124,125,131}I]FIAU and [^{124,125,131}I]FIRU was formulated in a saline solution. The chemical structures of [^{124,125,131}I]FIAU and [^{124,125,131}I]FIRU nucleoside analogues are shown in Figure 3.

Table 3. HPLC conditions for preparation of [$^{124.125,131}$I]FIAU and [$^{124.125,131}$I]FIRU

Number	Time (min)	Flow rate (mL/min)	D. W. + 0.1% TFA (%)	100% Ethanol + 0.1% TFA (%)
0	0	2	95	5
1	1-5	2	95	5
2	5-15	2	20	80
3	15-20	2	20	80
4	20-25	2	95	5
5	25-35	2	95	5

* TFA; trifluoroacetic acid

A) [^{124,125,131}I]FIAU

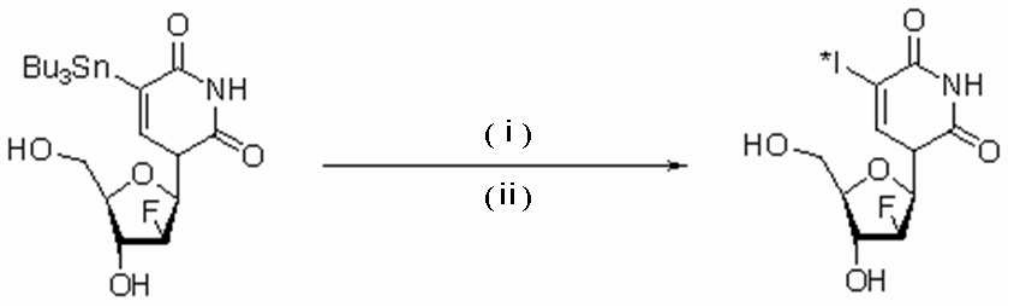

(i) Na[*I], 0.01 N NaOH, EtOH,

(ii) 1.0 N HCl to pH 4.0-5.0, 30 % H_2O_2, 30 min

B) [^{124,125,131}I]FIRU

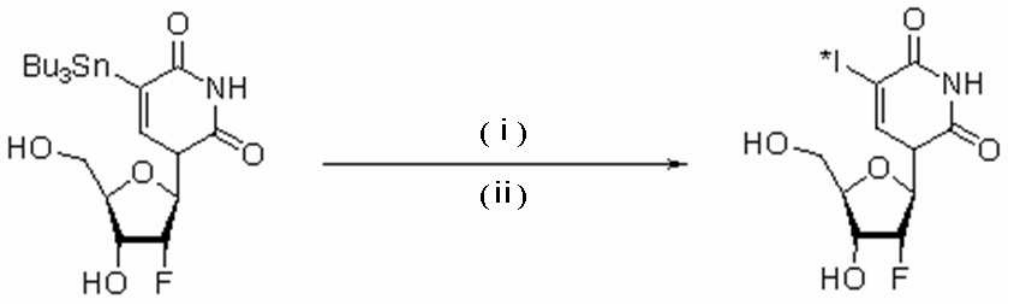

(i) Na[*I], 0.01 N NaOH, EtOH,

(ii) 1.0 N HCl to pH 4.0-5.0, 30 % H_2O_2, 30 min

Figure 3. The radio-labeling and chemical structure of [^{124,125,131}I]FIAU and [^{124,125,131}I]FIRU. Radiochemical purity of FIAU and FIRU was >99%.

3. Cell line and culture

MCA and MCA-TK cells were grown in Dulbecco's modified eagle's medium (DMEM; Welgene, Seoul, Korea) supplemented with 20% horse serum (Gibco, Carlsbad, USA), 5% fetal bovine serum (FBS; JHR Biosciences, Lenexa, USA) and 1% penicillin-streptomycin (Gibco, Carlsbad, USA). Medium was changed twice or three times a week. The cells were cultured at 37℃ in a 5 % CO_2 atmosphere. The MCA-TK cell line was selected in the presence of G418 (600 ㎍/mL; Gibco, Carlsbad, USA).

4. Assays for cytotoxcicity and cell proliferation

MCA and MCA-TK cells (2×10^3 cells/50 μL) were seeded into 96-well plates. GCV (Sigma, St. Louis, USA), iodinated FIAU, or iodinated FIRU was added to each well (0-10 mM/0.1 mL). After incubation for 5 days at 37℃ under 5% CO_2, MTS was added to each well (317 μg/mL). Following an additional 2 h incubation, proliferation of the treated cells were quantified by measuring the absorbance of culture media at 492 nm with a 96-well plate reader (GENios, TECAN Co., Boston, USA). Reference wavelength was quantified by absorbance at 650 nm.

The cytotoxicities of FIAU and FIRU were compared to each other, which have different sugar ring structure from each other. GCV was used as a standard reference nucleoside analog. For preparation of GCV, FIAU, or FIRU solution, the nucleoside analogues were solubilized in dimethyl sulfoxide (DMSO; Sigma, St. Louis, USA) to reach 5% concentration. The nucleoside analogue solutions were diluted with cell culture media to reach 5% DMSO concentration. The trypan blue dye (Sigma, St. Louis, USA) exclusion assay was used in conjunction with examination of cellular density using a hemocytometer. All experiments were performed in triplicate.

5. Cellular uptakes of radioactive iodine-labeled FIAU and FIRU

MCA and MCA-TK cells were plated in 6-well plates at a density of 5×10^5 cells/well and incubated at 37℃ for 24 h. When reached 80-100% confluence, each well was incubated with [^{125}I]FIAU and [^{125}I]FIRU (1 μCi/2 mL) for 0.5, 1, 2, and 4 h at 37 ℃ under 5% CO_2 atmosphere. The cells rinsed three times with Dulbecco's phosphate-buffered saline without Mg^{2+} and Ca^{2+} (Welgene, Seoul, Korea), and adherent cells were harvested. The radioactivity of harvested cells was determined by γ-counter (PerkinElmer, Waltham, USA). The radioactivities of triplicated samples were measured at designated time points. The accumulation of radiotracers was calculated as the percentage of the tracer dose added to the medium.

6. Subcutaneously and intravenously xenografted nude mice as a tumor model

Five to six-weeks-old female BALB/c nu/nu mice (SLC, Hamamatsu, Japan) were used to establish a tumor model. MCA (1×10^6 cells) and MCA-TK cells (1×10^6 cells) suspended in 100 μL of serum-free cell culture medium were subcutaneously transplanted into both shoulders. In order to prepare a mouse model carrying two different xenografts, the transduced MCA-TK cells were transplanted in the right shoulder while wild-type MCA cells were transplanted in the left shoulder as a negative control in the same mouse. Tumor growth was assessed by measuring bidimensional diameters with calipers. The mice carrying subcutaneous tumors of a volume of approximately 1,000 mm^3 were used for *in vivo* imaging experiments.

To prepare metastatic tumor models, MCA (5×10^6 cells) and MCA-TK (5×10^6 cells) were injected into each mouse via the tail vein (n=3). After 4 h, 1 week, and 2 weeks post injection, γ-camera imaging was performed.

For *in vivo* trafficking images of [^{131}I]FIAU cellular uptakes, MCA and MCA-TK cells were incubated in 10 mL of the medium containing 1 mCi of [^{131}I]FIAU at 37℃ for 2.5 h. Then, the cells were centrifuged at 1,500 rpm for 3 min and washed twice. The cells were further cultured in the fresh medium for 20 h, harvested, and then resuspended in 0.2 mL volumes of phosphate-buffered saline for injection. The prepared MCA (3-5 × 10^6 cells) or MCA-TK (3-5 × 10^6 cells) were injected into mice via the tail vein.

7. Imaging of tumor-xenografted mice with a microPET and a γ-camera

The tumor size reached a volume of 1000 mm^3 at approximately 3 weeks after subcutaneous implantation. [^{124,131}I]FIAU or [^{124,131}I]FIRU were administered to mice carrying the tumors through the tail vein. The mice were placed in a spread-supine position on a warm-bed slat.

The mice were anesthetized with 2% isoflurane (Choongwae, Seoul, Korea) before the injection of [^{124,131}I]FIAU and [^{124,131}I]FIRU and 1.5% isoflurane during all scanning time for imaging. For thyroid-blocked images, the mice were intraperitoneally injected with 1 mg of sodium perchlorate (Sigma, St. Louis, USA) before i.v. injection of [^{124,131}I]FIAU and [^{124,131}I]FIRU.

MicroPET images were obtained using a microPET system (microPET-R4; Concorde Microsystems, Inc., Knoxville, USA). Images were acquired at 1 h, 3 h, 5 h, 8 h, 12 h, 24 h, 48 h, and 132 h after injection of [^{124}I]FIAU or [^{124}I]FIRU (approximately 300 μCi/mouse). Each image was obtained for 30 min at the designated time points. The acquired images were reconstructed according to pre-determined calibration factors.

The γ-camera (Emission computed tomography; ZLC3700S, Siemens, Munich, Germany) images of mice were scanned at various time points after injection of [^{131}I]FIAU or [^{131}I]FIRU (approximately 300 μCi/mouse). The γ-camera images were acquired up to 200,000 counts with the pinhole collimators having a focal length of 9 cm and a diameter of 4 mm. All of the images were reconstructed with a correction for center-of rotation error. The γ-camera was fitted with a high-energy high-resolution collimator and a 364 KeV photopeak energy window for [^{131}I].

For imaging of metastasized tumors, at the designated time points [^{131}I]FIAU (approximately 200 μCi) was injected to the mice intravenously

implanted with MCA-TK cells. Images with γ-camera were taken at 24 h post injection.

For cell trafficking images, MCA and MCA-TK cells, which are incubated with [^{131}I]FIAU, were injected into the mice via the tail vein and γ-camera images were taken at 30 min, 6 h, 24 h, 48 h, and 72 h post injection. One week later, [^{131}I]FIAU (approximately 200 μCi) was re-injected through the tail vein in the same mouse, and γ-camera images was taken at 5 h and 30 h post injection.

8. Image analysis

Images analysis was performed with quantification of [^{124}I] retention in HSV1-TK expression regions. The value of %ID/g was estimated from the acquired PET images with pre-determined calibration factors in the region of interest (ROI) placed on tumors. The ratio of MCA-TK to MCA tumor region %ID/g and MCA-TK to muscle %ID/g were calculated.

$$\%ID/g = \frac{[\text{count/pixel (uCi/cc)}] \times [\text{CCF (cc/g)}]}{[\text{injected dose (uCi)}]}$$

The cross calibration factor (CCF) was applied to make accurate observations. The CCF was 1 in this experiment.

Ⅲ. RESULTS

1. Radiolabeling of FIAU and FIRU

Radiolabeling of the FIAU and FIRU with $^{124}I^-$ $^{125}I^-$ and ^{131}I were successfully achieved by the iododestannylation reaction in good yields (60-80%) (Fig. 4). Radiochemical purity of the compounds was <98%.

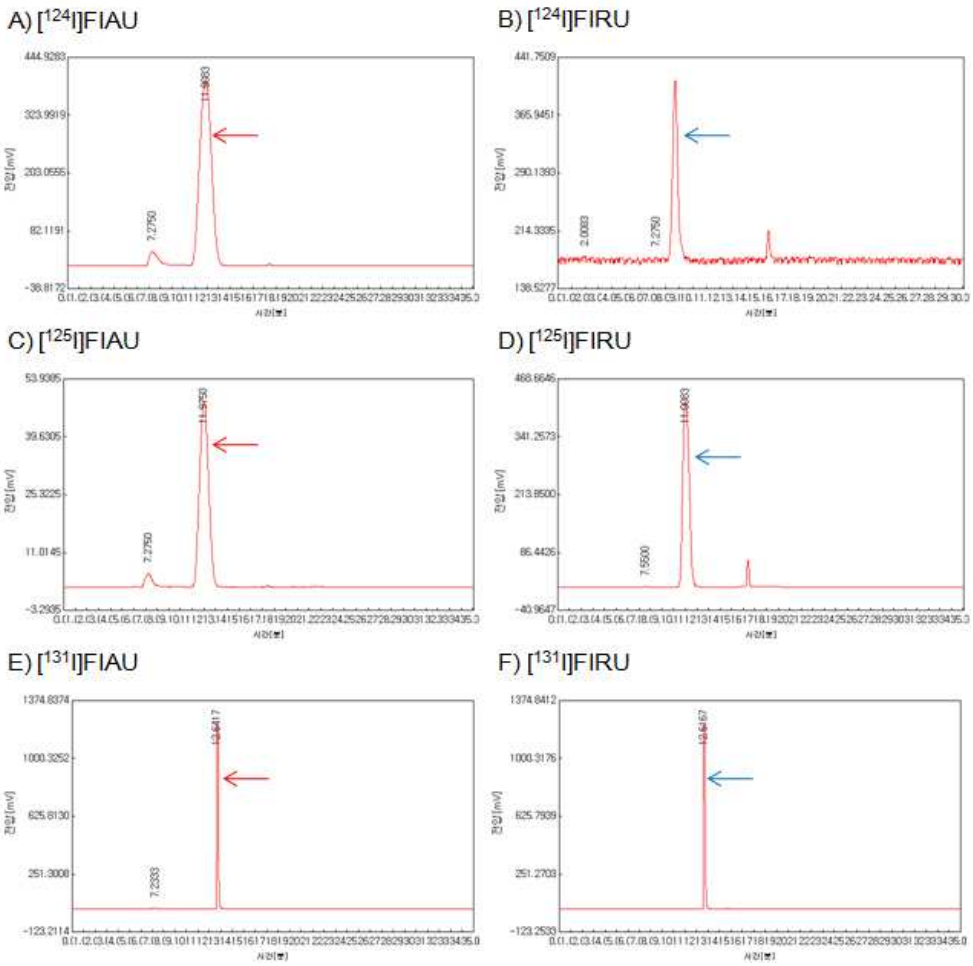

Figure 4. Reverse phase chromatography elution profile of [^{124,125,131}I]FIAU and [^{124,125,131}I]FIRU. (C-18 column, 3.9 mm × 300 mm, EtOH/H_2O = 5:95 (0 min) to 8:2 (20 min) [v/v], flow rate: 2.0 mL/min)

2. Cytotoxicities of non-radiolabeled nucleoside analogues

The cytotoxicities (IC_{50}) of GCV and its iodinated analoques, FIAU and FIRU, were examined by the MTS method. In MCA-TK cells, IC_{50} range of various compounds was from 1.026×10^{-3} to 7.271×10^{-8} M (Figure 5 and Table 4).

FIAU (IC_{50}, 7.271×10^{-8} M) was shown to be more toxic than FIRU (IC_{50}, 1.026×10^{-3} M) in MCA-TK cells. FIRU was much less toxic than GCV (IC_{50}, 4.443×10^{-8} M) in the same cells. The same compounds exhibited less cytotoxicities to MCA cells, compared with MCA-TK cells. IC_{50} of the dissolving solution (DMSO) was 1.292×10^{-2} M in MCA-TK and 1.016×10^{-2} M in MCA cells.

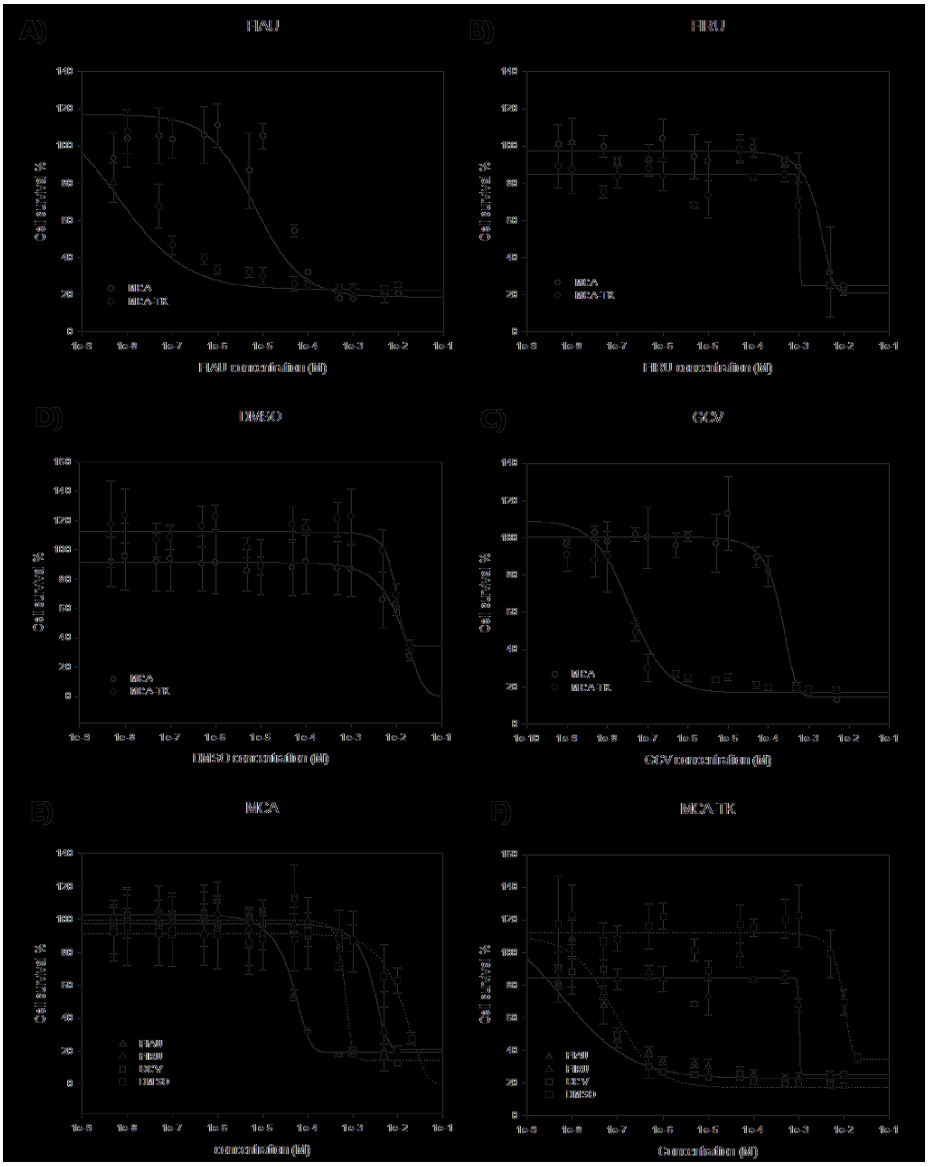

Figure 5. Cytotoxicity of FIAU, FIRU, GCV and DMSO in MCA and MCA-TK cells. Cytotoxicities of FIAU (A), FIRU (B), DMSO(C), and GCV (D) in MCA and MCA-TK cells were examined by the MTS assay. The same experimental results were represented in MCA cells (E) and MCA-TK cells (F).

Table 4. IC_{50} of nucleoside analogues of FIAU, FIRU, GCV and DMSO in MCA and MCA-TK cells

Cell lines	Nucleoside analogues (M)			Dissolving solution (M)
	FIAU	FIRU	GCV*	DMSO**
MCA	2.735×10^{-5}	2.521×10^{-3}	1.569×10^{-4}	1.016×10^{-2}
MCA-TK	7.271×10^{-8}	1.026×10^{-3}	4.443×10^{-8}	1.292×10^{-2}

*GCV; standard analogue of cytotoxicity of HSV1-TK gene expression cells.

**DMSO; dissolving solution of FIAU, FIRU and GCV

3. Cellular uptakes of [^{125}I]FIAU and [^{125}I]FIRU

Figure 6 shows the results of selective uptake and retention of [^{125}I]FIAU and [^{125}I]FIRU by MCA-TK cells as compared with those of the parental MCA cells. Generally, uptake of the radiolabelled nucleoside analogues by MCA-TK cells was higher than that by MCA cells.

Cellular uptake of [^{125}I]FIAU was continuously increased according to the length of incubation time in both MCA and MCA-TK cells. Meanwhile, cellular uptake of [^{125}I]FIRU in MCA-TK cells was the highest at 2 hour's incubation and then decreased at 4 hour's incubation in both MCA and MCA-TK cells. In MCA-TK cells, [^{125}I]FIAU accumulation was higher than [^{125}I]FIRU.

The highest ratio of [^{125}I]FIAU accumulation in the MCA-TK cells and that in the MCA cells was about 100 at 1 hour's incubation. At 4 hour's incubation, the ratio of [^{125}I]FIAU accumulations in the both cell lines was about 19.7. Meanwhile, the ratio of [^{125}I]FIRU accumulations in the both cell lines (374.4) was much higher than [^{125}I]FIAU (19.7) at 4 hour's incubation. These data of accumulation ratio in the MCA-TK and MCA cells showed that [^{125}I]FIRU was able to be more selectively taken up and more effectively remain in the cells than [^{125}I]FIAU.

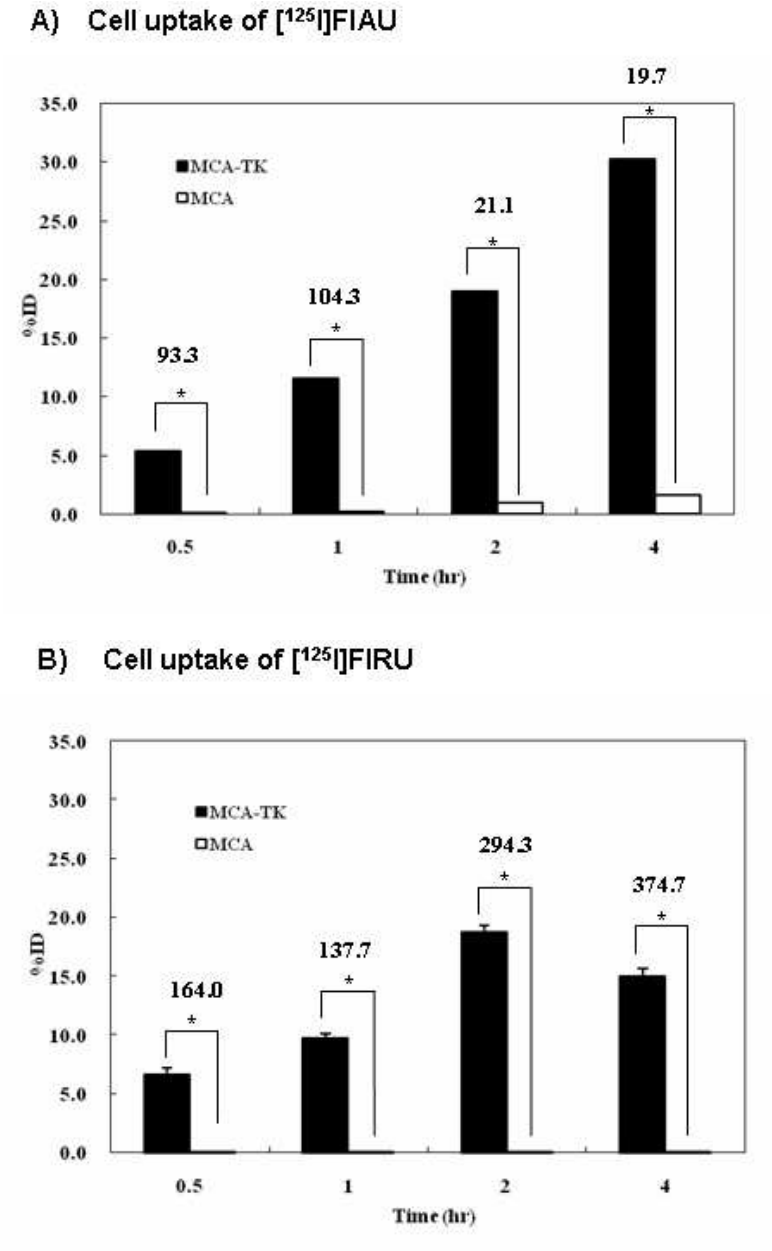

Figure 6. Cellular uptakes of [^{125}I]FIAU and [^{125}I]FIRU by MCA and MCA-TK cells. Uptakes of [^{125}I]FIAU (A) and [^{125}I]FIRU (B) by MCA and MCA-TK cells were measured after incubation for 0.5, 1, 2, and 4 h. %ID: percentage of injected dose. *%ID ratios of [^{125}I]FIAU and [^{125}I]FIRU uptakes in MCA-TK and MCA cells.

4. γ-camera images of MCA and MCA-TK tumors in mice

For *in vivo* γ-camera imaging, 300 μCi of [^{131}I]FIAU or [^{131}I]FIRU was intravenously injected into the mice carrying MCA or MCA-TK tumors. In the mice carrying MCA-TK tumors, intratumoral accumulation of [^{131}I]FIAU was localized until 288 h post injection (Figure 7A). Accumulation of [^{131}I]FIAU in MCA tumors was significantly lower than that in MCA-TK tumors. The accumulation of [^{131}I]FIAU in MCA tumors disappeared in 20 h post injection as the body background diminished.

At beginning, effective accumulation of [^{131}I]FIRU in MCA-TK tumors was observed and clearly distinguished from that in MCA tumors (Figure 7B). [^{131}I]FIRU signal in the MCA-TK tumor region was seen only to 20 h post-injection. As [^{131}I]FIRU signal in the MCA-TK tumor region decreased, thyroid uptake of [^{131}I]FIRU increased, clearly seen at 20 h post injection. In addition, the body background of [^{131}I]FIRU was greater than that of [^{131}I]FIAU and slowly diminished.

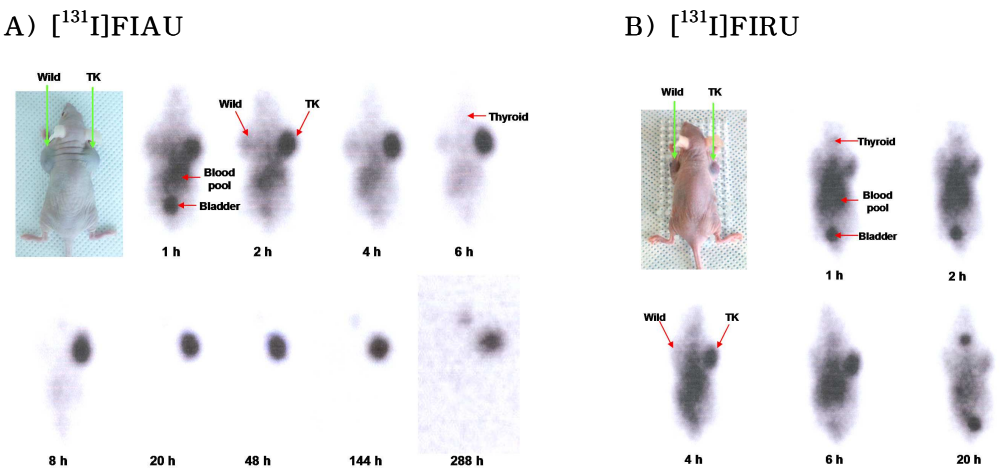

Figure 7. Planar ɣ-camera images of mice carrying MCA-TK or MCA tumors after injection of [^{124}I]FIAU and [^{124}I]FIRU. MCA-TK tumors were implanted in the right shoulder of a thyroid blocked nude mouse and control MCA tumors were in the left shoulder. (A) For HSV1-TK-targeted imaging, [^{131}I]FIAU was administered 300 μCi into mice via tail vein. After 1 h, 2 h, 4 h, 6 h, 8 h, 20 h, 48 h, 144 h and 288 h post-injection, ɣ-camera imaging was performed in a spread-supine position. (B) ɣ-camera images of HSV1-TK-expressing tumors were scanned at 1 h, 2 h, 4 h, 6 h and 20 h after [^{131}I]FIRU injection (300 μCi) via tail vein.

5. MicroPET images of MCA and MCA-TK tumors in mice

In the xenograft tumor model, intratumoral accumulations of [^{124}I]FIAU and [^{124}I]FIRU were examined by microPET imaging (Figure 8). First of all, the uptakes of [^{124}I]FIAU and [^{124}I]FIRU by MCA-TK tumors were far greater and more selective than those by MCA tumors. Accumulation of [^{124}I]FIAU or [^{124}I]FIRU in the MCA-TK tumors was clearly localized for first 12 h while radioactive images of the MCA tumors were not distinguished from the background images.

According to the serial microPET images of [^{124}I]FIAU in the MCA and MCA-TK tumors, [^{124}I]FIAU was more effectively and selectively taken up by the MCA-TK tumor cells for 132 h (Figure 8A). The same compound was little localized in the MCA tumor region. [^{124}I]FIAU localization in thyroid began to be seen in 48 h post injection and became further clear 132 h later. These data of *in vivo* [^{124}I]FIAU uptakes by the MCA or MCA-TK tumors were consistent with the previous *in vitro* data of cellular uptakes (Figure 6).

[^{124}I]FIRU uptake by the MCA or MCA-TK tumors was monitored for 48 h after injection (Figure 8B). Although the background signals were elevated, uptakes of [^{124}I]FIRU by the MCA and MCA-TK tumors could be distinguished form the background signals. The uptake by the MCA-TK tumors was more significant than that by the MCA tumors and persisted for 48 h. The radioactive image in the MCA tumor area was disappeared in 24 h post injection. [^{124}I]FIRU was easily accumulated in the thyroid and its accumulation was increased with time passing. The microPET images of *in vivo* accumulation of [^{131}I]FIAU and [^{131}I]FIRU were similar to the previous γ-camera images (Figure 7).

A) [^{124}I]FIAU

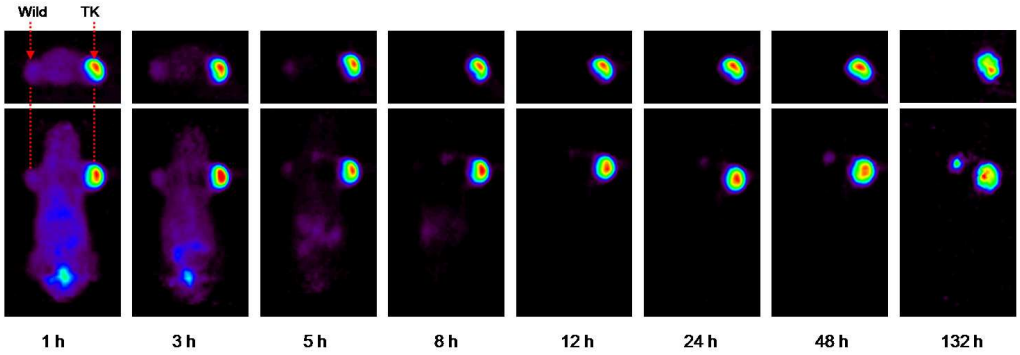

B) [^{124}I]FIRU

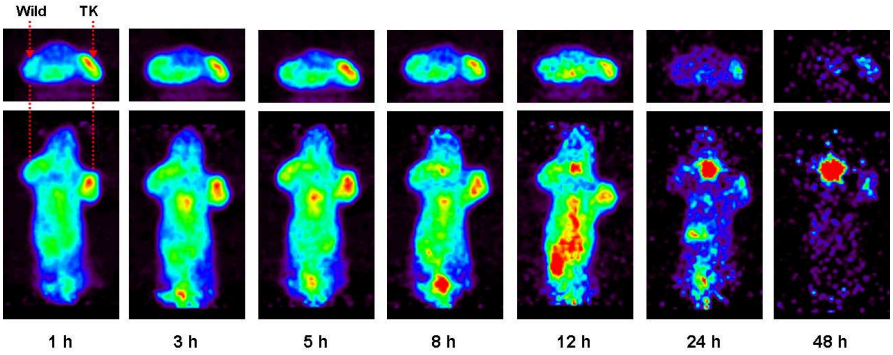

Figure 8. Representative serial microPET images of mice carrying MCA-TK or MCA tumors after injection of [^{124}I]FIAU and [^{124}I]FIRU. A series of microPET images of a thyroid blocked nude mouse carrying MCA-TK or MCA tumors were taken at various time points following tail vein injection of [^{124}I]FIAU (A) and [^{124}I]FIRU (B). The upper images are transverse images and the lower position images are coronal images. The MCA-TK tumors were in right shoulder; the control MCA tumors were in left shoulder.

6. Analysis of the microPET images

The amounts of [^{124}I]FIAU or [^{124}I]FIRU accumulated in MCA or MCA-TK tumors were calculated from the microPET images as %ID/g of ROIs (Table 6). ROI was placed on tumor regions in PET images and %ID/g was estimated by pre-determined calibration factors. In the MCA-TK tumor region, %ID/g of [^{124}I]FIAU was higher than that of [^{124}I]FIRU. And, %ID/g of [^{124}I]FIAU was about 146.0 at 24 h.

In the case of [^{124}I]FIAU, radioactivity accumulation in the tumors was continuously decreased for 132 h. However, the ratios of %ID/g in MCA-TK tumors was increased for 48 h at which the ratio of %ID/g was the highest, 187.3.

Changes of %ID/g of [^{124}I]FIRU in the MCA and MCA-TK tumors was similar to those of [^{124}I]FIAU. According to the calculation from the microPET images, the %ID/g ratios of [^{124}I]FIRU accumulation in the MCA-TK and MCA tumors for 48 h was relatively constant, approximately 1.5. The ratios of [^{124}I]FIAU accumulations in the MCA-TK tumors and in muscle was higher than those of [^{124}I]FIRU. For example, at 24 h post injection the %ID/g ratio of [^{124}I]FIRU was 793.0 while that of [^{124}I]FIRU was only 2.2.

Table 5. The %ID/g of [^{124}I]FIAU and [^{124}I]FIRU in mice bearing MCA-TK or MCA tumors

Time (h)	%ID/g[¶] of [^{124}I]FIAU					%ID/g[¶] of [^{124}I]FIRU				
	MCA	MCA-TK	MCA-TK/MCA[†]	Muscle	MCA-TK/Muscle[‡]	MCA	MCA-TK	MCA-TK/MCA[†]	Muscle	MCA-TK/Muscle[‡]
1	2.05	9.96	4.85	1.30	7.66	5.09	6.46	1.27	2.12	3.05
3	1.08	9.10	8.39	0.28	32.50	4.10	5.51	1.34	2.14	2.57
5	0.49	8.41	17.28	0.12	70.08	3.29	4.07	1.24	1.64	2.48
8	0.14	8.19	57.31	0.06	136.50	1.68	2.37	1.41	0.98	2.42
12	0.06	7.45	117.86	0.02	372.50	0.85	1.20	1.40	0.42	2.86
24	0.05	7.11	146.01	0.01	711.00	0.10	0.15	1.54	0.07	2.14
48	0.03	5.08	187.31	0.01	508.00	0.01[§]	0.04[§]	4.00	0.01	4.00
132	0.01	1.72	135.64	0.01	172.00	-	-	-	-	-

[¶]%ID/g (percentage of injected dose per gram of tissue) was calculated from radioactive ROI (region of interest) areas in microPET images.
[†]Ratios of %ID/g in MCA-TK to MCA tumors
[‡]Ratios of %ID/g in MCA-TK tumor to muscle
[§]Tumor regions of microPET images were not clear.

7. Imaging of *in vivo* tumor cell trafficking and metastasized tumors

For imaging of [^{131}I]FIAU-containing cell trafficking with γ-camera, the MCA and MCA-TK cells were treated with [^{131}I]FIAU for 2.5 h and then incubated for additional 20 h in the absence of [^{131}I]FIAU. The [^{131}I]FIAU-treated cells were administered to mice via the tail vein. The MCA-TK cells retaining [^{131}I]FIAU were predominantly accumulated in the lungs up to 6 h and then dissipated (Figure 9A). Meanwhile, the MCA cells exhibited the accumulation in the lungs only for 30 min and earlier dissipation.

One week later, the MCA or MCA-TK cells retaining [^{131}I]FIAU were reinjected into the same mice. The both cell types showed a low level of accumulation in the mice at 5 h and 30 h post injection (Figure 9B).

For imaging of metastasized MCA-TK tumor cells, [^{131}I]FIAU was intravenously administered into the mice preinjected with MCA-TK cells in 4 h-2 weeks advance. The i.v. administration of [^{131}I]FIAU at 2 weeks post injection of tumor cells was not able to localize the metastasized tumors in the body (Figure 9C). However, the [^{131}I]FIAU uptakes in the thyroid was seen after 24 h post injection.

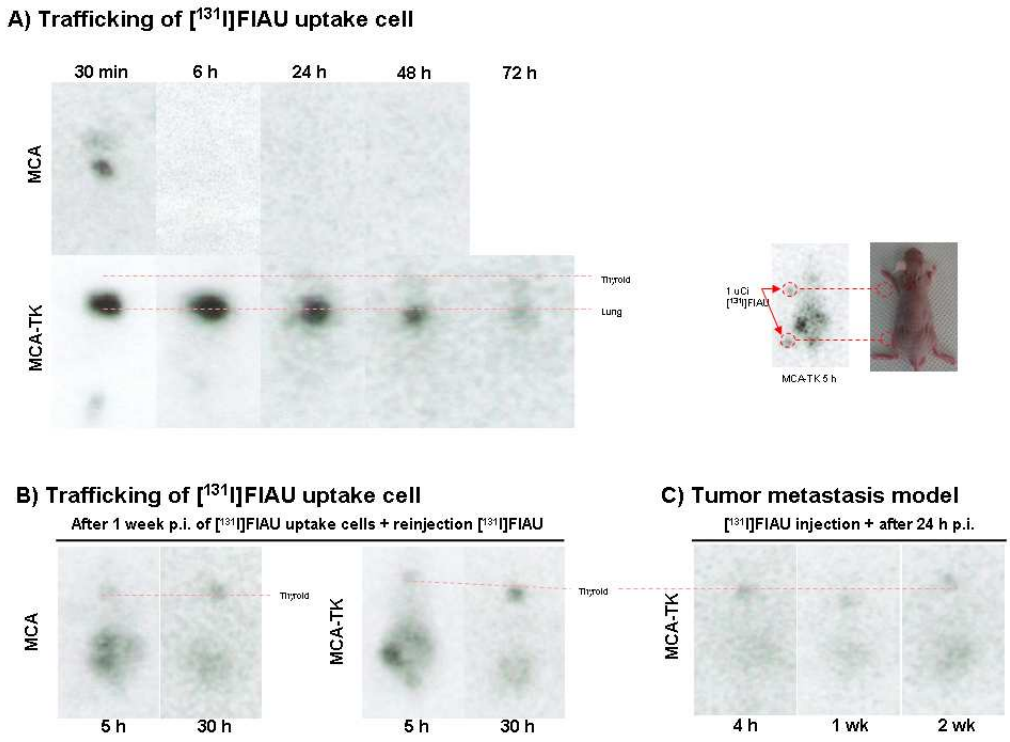

Figure 9. Serial γ-camera imaging of MCA and MCA-TK cell trafficking and metastasized tumors. (A) For imaging of trafficking cells, mice were intravenously injected with MCA or MCA-TK cells retaining [^{131}I]FIAU. After 30 min, 6 h, 24 h, 48 h, and 72 h post injection, γ-camera imaging was performed in a spread-supine position. (B) One week later, the tumor cells retaining [^{131}I]FIAU were injected to the previously injected same mouse and γ-camera imaging was performed 5 h and 30 h later. (C) For imaging of metastasized tumors, the MCA-TK cells were intravenously injected into mice. After 4 hours, 1 week, and 2 weeks post injection of the MCA-TK cells, γ-camera imaging was performed after 24 h post injection of [^{131}I]FIAU.

Ⅳ. DISCUSSION

A specific research aim in this thesis is to assess the effects of the structural difference of FIAU and FIRU, which have a different 2′-fluoro configuration, on their functioning as a tracing agent for *in vivo* imaging. It has been suggested that placement of fluorine within the deoxyribose sugar stabilizes the glycosidic bond and lead not to be readily cleaved by thymidine phosphorylase [22, 42]. Also, before phosphorylation of nucleoside analogues, HSV1-TK enzyme is recognized primarily by nucleoside sugar pucker, sugar geometry that is defined by the five endocyclic torsion angles, for phosphorylation of nucleoside analogues [18, 20, 37, 43]. Sugar pucker of FIAU and FIRU is different because of each analogues have a configuration of arabino and ribo 2′-fluorine position.

In this study, biological functions of FIAU and FIRU as a potential tracer were compared for *in vivo* imaging of TK-expressing cells, such as MCA-TK tumors. The labeling of FIAU and FIRU with [^{124,125,131}I] was achieved in a high yield (60-80%) and high purity. A major advantage of using [^{124,125,131}I]-labeled probe is that the long half-life of radioactive-iodine allows repetitive and sequential image acquisition after injection. The radiolabeled FIAU and FIRU were effectively accumulated in the tumor cells expressing HSV1-TK (MCA-TK cells) in a tumor xenograft model.

The data of *in vitro* cytotoxicity analysis showed that FIAU was more cytotoxic to the both MCA and MCA-TK cell lines than FIRU. This implies that FIAU may be a better substrate of nucleoside analogue for DNA synthesis. The incorporation of nucleoside analogues into the DNA by DNA polymerases results in replication of unnatural DNA which induces cell death [43]. Presumably, the less toxicity of FIRU may be due to inefficient incorporation into the DNA.

The data of cytotoxicities and cellular uptakes of FIAU and FIRU indicate that their cytotoxicities do not depend on initial metabolic trapping, but on elaboration to more cytotoxic anabolites.

According to the cellular uptake data, [^{125}I]FIAU can be effectively taken up by the cell expressing thymidine kinases which phosphorylate FIAU in turn. Moreover, [^{125}I]FIRU also exhibited thymidine kinase-dependent uptake in MCA-TK cells. The radiolabeled FIAU uptake by the MCA-TK cells was increased continuously for 4 h while the accumulation of radiolabeled FIRU was decreased at the time point of 4 h. This result indicates that FIAU is more selectively accumulated in MCA-TK cells than FIRU. Meanwhile, the both compounds showed relatively lower uptake in MCA cells. This means that mammalian TK is not able to effectively intake non-natural nucleosides such as FIAU and FIRU as a substrate. The FIAU taken up by HSV1-TK-expressing cells is readily phosphorylated, followed by being incorporated into nucleic acids. Meanwhile, FIRU was also phosphorylated inside cell, but not metabolically elaborated into nucleic acids as previously suggested [44].

In a number of previous studies [10, 17, 23, 24, 28, 36], it has already been demonstrated that the radiolabeled FIAU is a suitable substrate for *in vivo* imaging of tumor cells expressing HSV1-TK. In this study, microPET images using [^{124}I]FIAU were acquired up to 132 h and γ-camera images using [^{131}I]FIAU were aquired up to 288 h. According to the *in vivo* imaging, dehalogenation of [^{124,131}I]FIAU seemed to be slow in the MCA-TK tumor models. This result demonstrates that [^{124,131}I]FIAU is more stable in terms of radioiodination stability in the *in vivo* tumor model. According to the microPET imaging data, the two different imaging agents of FIAU and FIRU yielded different patterns of body background in mice carrying MCA and MCA-TK tumors. [^{124}I]FIRU produced a higher background level throughout the body.

Meanwhile, highly specific and clear images of MCA-TK tumors were obtained by treatment with [^{124}I]FIAU. On the other hand, the γ-camera images showed that radiolabeled FIAU and FIRU were washed out more quickly from the MCA tumors and mouse body. Thyroid blocking with sodium perchlorate prior to injection of the radiolabeled FIAU and FIRU gave an advantage to acquire distinct images of microPET and γ-camera.

In this study, the microPET imaging shows that [^{124}I]FIAU is a better agent for imaging of cells expressing HSV1-TK than [^{124}I]FIRU. This result can be related to previous reports that [^{124,131}I]FIAU could be a useful derivative in imaging of stem cells [45, 46] and immunocytes [29, 47-49] because of its stability and capacity for long term image *in vivo*.

In a previous report, [^{124,131}I]FIRU was suggested as a candidate agent for molecular imaging, but its retention time in HSV1-TK-expressing tumors was not persisted [25]. The high levels of radioactivity in the kidneys implied the rapid clearance of [^{124,131}I]FIRU. In this study, [^{124,131}I]FIRU was continuously accumulated in the thyroid as time elapsed. The high radioactive images in thyroid represented the instability of [^{124,131}I]FIRU *in vivo*. Also, this data suggested that although FIRU could be transported into the cells and phosphorylated, it was not a good substrate for DNA polymerases. Hence, FIRU would be released out of cells as time elapsed.

Trafficking of cells expressing HSV1-TK was imaged using a γ-camera. The intravenously administered MCA-TK cells retaining [^{131}I]FIAU was heavily accumulated in the lungs. However, [^{131}I]FIAU reinjected one week later was accumulated little in the lungs, but more rapidly cleared from the body. The rapid clearance of the reinjected FIAU may be due to immune stimulation by the previously administered tumor cells. In the some studies [50-53], transplantation of pancreatic islet cells elicited instant blood-mediated inflammatory reaction (IBMIR), a type of innate inflammatory reaction.

Intraportally administered islets are subjected to this reaction, resulting in activation of platelets, neutrophils, and monocytes, as well as activation of the coagulation and complement systems.

Up to 2 weeks post injection of MCA-TK tumor cells, metastasized tumors was not localized by γ-camera imaging. There could be some speculations on the negative imaging. Firstly, 2 weeks may be not long enough for metastasized tumor cells to grow to large colonies which can be imaged by γ-camera. Secondly, MCA-TK cells may have a low metastatic potential, rendering low extravesation to other organs.

In this research, the radiolabeled FIAU showed more selectively and preferentially uptake by the tumor cells expressing HSV1-TK, MCA-TK. Therefore, it can be suggest that FIAU, the nucleoside analogue with fluorine in the 2′ positions of arabino-configuration, is a more suitable substrate for HSV1-TK and an appropriate agent for HSV1-TK-mediated imaging.

Ⅴ. REFERENCES

1. Pike, L., Petravicz, J., Wang, S., Bioluminescence imaging after HSV amplicon vector delivery into brain. J Gene Med, 2006. 8(7): p. 804-13.
2. Serganova, I., Ponomarev, V., Blasberg, R., Human reporter genes: potential use in clinical studies. Nucl Med Biol, 2007. 34(7): p. 791-807.
3. Serganova, I., Blasberg, R. G., Multi-modality molecular imaging of tumors. Hematol Oncol Clin North Am, 2006. 20(6): p. 1215-48.
4. Massoud, T.F., Singh, A., Gambhir, S. S., Noninvasive molecular neuroimaging using reporter genes: part I, principles revisited. AJNR Am J Neuroradiol, 2008. 29(2): p. 229-34.
5. Haberkorn, U., Altmann, A., Imaging methods in gene therapy of cancer. Curr Gene Ther, 2001. 1(2): p. 163-82.
6. Gambhir, S.S., Barrio, J. R., Herschman, H. R., Phelps, M. E., Imaging gene expression: principles and assays. J Nucl Cardiol, 1999. 6(2): p. 219-33.
7. Yan, L., Han, Y., He, Y., Xie, H., Liu, J., Zhao, L., Wang, J., Gao, L., Fan, D., , Cell tracing techniques in stem cell transplantation. Stem Cell Rev, 2007. 3(4): p. 265-9.
8. Yang, M., Baranov, E., Moossa, A. R., Penman, S., Hoffman, R. M., Visualizing gene expression by whole-body fluorescence imaging. Proc Natl Acad Sci U S A, 2000. 97(22): p. 12278-82.
9. Sun, X., Annala, A. J., Yaghoubi, S. S., Barrio, J. R., Nguyen, K. N., Toyokuni, T., Satyamurthy, N., Namavari, M., Phelps, M. E., Herschman, H. R., Gambhir, S. S., Quantitative imaging of gene induction in living animals. Gene Ther, 2001. 8(20): p. 1572-9.
10. Tjuvajev, J.G., Chen, S. H., Joshi, A., Joshi, R., Guo, Z. S., Balatoni, J.,

Ballon, D., Koutcher, J., Finn, R., Woo, S. L., Blasberg, R. G., Imaging adenoviral-mediated herpes virus thymidine kinase gene transfer and expression in vivo. Cancer Res, 1999. 59(20): p. 5186-93.

11. Ray, P., Bauer, E., Iyer, M., Barrio, J. R., Satyamurthy, N., Phelps, M. E., Herschman, H. R., Gambhir, S. S., Monitoring gene therapy with reporter gene imaging. Semin Nucl Med, 2001. 31(4): p. 312-20.

12. Green, L.A., Nguyen, K., Berenji, B., Iyer, M., Bauer, E., Barrio, J. R., Namavari, M., Satyamurthy, N., Gambhir, S. S., A tracer kinetic model for 18F-FHBG for quantitating herpes simplex virus type 1 thymidine kinase reporter gene expression in living animals using PET. J Nucl Med, 2004. 45(9): p. 1560-70.

13. Cai, H., Yin, D., Zhang, L., Yang, X., Xu, X., Liu, W., Zheng, X., Zhang, H., Wang, J., Xu, Y., Cheng, D., Zheng, M., Han, Y., Wu, M., Wang, Y., Preparation and biological evaluation of 2-amino-6-[18F]fluoro-9-(4-hydroxy-3-hydroxy-methylbutyl) purine (6-[18F]FPCV) as a novel PET probe for imaging HSV1-tk reporter gene expression. Nucl Med Biol, 2007. 34(6): p. 717-25.

14. Urbain, J.L., Reporter genes and imagene. J Nucl Med, 2001. 42(1): p. 106-9.

15. Gambhir, S.S., Barrio, J. R., Herschman, H. R., Phelps, M. E., Assays for noninvasive imaging of reporter gene expression. Nucl Med Biol, 1999. 26(5): p. 481-90.

16. Iyer, M., Sato, M., Johnson, M., Gambhir, S. S., Wu, L., Applications of molecular imaging in cancer gene therapy. Curr Gene Ther, 2005. 5(6): p. 607-18.

17. Choi, S.R., Zhuang, Z. P., Chacko, A. M., Acton, P. D., Tjuvajev-Gelovani, J., Doubrovin, M., Chu, D. C., Kung, H. F., SPECT imaging of herpes simplex virus type1 thymidine kinase gene expression

by [(123)I]FIAU(1). Acad Radiol, 2005. 12(7): p. 798-805.

18. Tae, E.L., Wu, Y., Xia, G., Schultz, P. G., Romesberg, F. E., Efforts toward expansion of the genetic alphabet: replication of DNA with three base pairs. J Am Chem Soc, 2001. 123(30): p. 7439-40.

19. Marquez, V.E., Ben-Kasus, T., Barchi, J. J., Jr., Green, K. M., Nicklaus, M. C., Agbaria, R., Experimental and structural evidence that herpes 1 kinase and cellular DNA polymerase(s) discriminate on the basis of sugar pucker. J Am Chem Soc, 2004. 126(2): p. 543-9.

20. Marquez, V.E., Choi, Y., Comin, M. J., Russ, P., George, C., Huleihel, M., Ben-Kasus, T., Agbaria, R., Understanding how the herpes thymidine kinase orchestrates optimal sugar and nucleobase conformations to accommodate its substrate at the active site: a chemical approach. J Am Chem Soc, 2005. 127(43): p. 15145-50.

21. Alauddin, M.M., Shahinian, A., Park, R., Tohme, M., Fissekis, J. D., Conti, P. S., In vivo evaluation of 2′-deoxy-2′-[(18)F]fluoro-5-iodo-1-beta-D-arabinofuranosyluracil ([18F]FIAU) and 2′-deoxy-2′-[18F]fluoro-5-ethyl-1-beta-D-arabinofuranosyluracil ([18F]FEAU) as markers for suicide gene expression. Eur J Nucl Med Mol Imaging, 2007. 34(6): p. 822-9.

22. Mankoff, D.A., Shields, A. F., Krohn, K. A., PET imaging of cellular proliferation. Radiol Clin North Am, 2005. 43(1): p. 153-67.

23. Tjuvajev, J.G., Stockhammer, G., Desai, R., Uehara, H., Watanabe, K., Gansbacher, B., Blasberg, R. G., Imaging the expression of transfected genes in vivo. Cancer Res, 1995. 55(24): p. 6126-32.

24. Tjuvajev, J.G., Finn, R., Watanabe, K., Joshi, R., Oku, T., Kennedy, J., Beattie, B., Koutcher, J., Larson, S., Blasberg, R. G., Noninvasive imaging of herpes virus thymidine kinase gene transfer and expression: a potential

method for monitoring clinical gene therapy. Cancer Res, 1996. 56(18): p. 4087-95.

25. Nanda, D., de Jong, M., Vogels, R., Havenga, M., Driesse, M., Bakker, W., Bijster, M., Avezaat, C., Cox, P., Morin, K., Naimi, E., Knaus, E., Wiebe, L., Smitt, P. S., Imaging expression of adenoviral HSV1-tk suicide gene transfer using the nucleoside analogue FIRU. Eur J Nucl Med Mol Imaging, 2002. 29(7): p. 939-47.

26. Gambhir, S.S., Barrio, J. R., Phelps, M. E., Iyer, M., Namavari, M., Satyamurthy, N., Wu, L., Green, L. A., Bauer, E., MacLaren, D. C., Nguyen, K., Berk, A. J., Cherry, S. R., Herschman, H. R., Imaging adenoviral-directed reporter gene expression in living animals with positron emission tomography. Proc Natl Acad Sci U S A, 1999. 96(5): p. 2333-8.

27. Toyohara, J., Hayashi, A., Sato, M., Tanaka, H., Haraguchi, K., Yoshimura, Y., Yonekura, Y., Fujibayashi, Y., Rationale of 5-(125)I-iodo-4′-thio-2′-deoxyuridine as a potential iodinated proliferation marker. J Nucl Med, 2002. 43(9): p. 1218-26.

28. Wang, H.E., Yu, H. M., Liu, R. S., Lin, M., Gelovani, J. G., Hwang, J. J., Wei, H. J., Deng, W. P., Molecular imaging with 123I-FIAU, 18F-FUdR, 18F-FET, and 18F-FDG for monitoring herpes simplex virus type 1 thymidine kinase and ganciclovir prodrug activation gene therapy of cancer. J Nucl Med, 2006. 47(7): p. 1161-71.

29. Zanzonico, P., Koehne, G., Gallardo, H. F., Doubrovin, M., Doubrovina, E., Finn, R., Blasberg, R. G., Riviere, I., O'Reilly, R. J., Sadelain, M., Larson, S. M., [131I]FIAU labeling of genetically transduced, tumor-reactive lymphocytes: cell-level dosimetry and dose-dependent toxicity. Eur J Nucl Med Mol Imaging, 2006. 33(9): p. 988-97.

30. Mercer, J.R., Xu, L. H., Knaus, E. E., Wiebe, L. I., Synthesis and

tumor uptake of 5-82Br- and 5-131I-labeled 5-halo-1-(2-fluoro-2-deoxy-beta-D-ribofuranosyl)uracils. J Med Chem, 1989. 32(6): p. 1289-94.

31. Wiebe, L.I., E.E. Knaus, and K.W. Morin, Radiolabelled pyrimidine nucleosides to monitor the expression of HSV-1 thymidine kinase in gene therapy. Nucleosides Nucleotides, 1999. 18(4-5): p. 1065-6.

32. Alauddin, M.M., Shahinian, A., Kundu, R. K., Gordon, E. M., Conti, P. S., Evaluation of 9-[(3-18F-fluoro-1-hydroxy-2-propoxy)methyl]guanine ([18F]-FHPG) in vitro and in vivo as a probe for PET imaging of gene incorporation and expression in tumors. Nucl Med Biol, 1999. 26(4): p. 371-6.

33. Jacobs, A., Tjuvajev, J. G., Dubrovin, M., Akhurst, T., Balatoni, J., Beattie, B., Joshi, R., Finn, R., Larson, S. M., Herrlinger, U., Pechan, P. A., Chiocca, E. A., Breakefield, X. O., Blasberg, R. G., Positron emission tomography-based imaging of transgene expression mediated by replication-conditional, oncolytic herpes simplex virus type 1 mutant vectors in vivo. Cancer Res, 2001. 61(7): p. 2983-95.

34. Meltzer, C.C., Kondziolka, D., Villemagne, V. L., Wechsler, L., Goldstein, S., Thulborn, K. R., Gebel, J., Elder, E. M., DeCesare, S., Jacobs, A., Serial [18F] fluorodeoxyglucose positron emission tomography after human neuronal implantation for stroke. Neurosurgery, 2001. 49(3): p. 586-91; discussion 591-2.

35. Jacobs, A., Voges, J., Reszka, R., Lercher, M., Gossmann, A., Kracht, L., Kaestle, C., Wagner, R., Wienhard, K., Heiss, W. D., Positron-emission tomography of vector-mediated gene expression in gene therapy for gliomas. Lancet, 2001. 358(9283): p. 727-9.

36. Tjuvajev, J.G., Avril, N., Oku, T., Sasajima, T., Miyagawa, T., Joshi, R., Safer, M., Beattie, B., DiResta, G., Daghighian, F., Augensen, F.,

Koutcher, J., Zweit, J., Humm, J., Larson, S. M., Finn, R., Blasberg, R., Imaging herpes virus thymidine kinase gene transfer and expression by positron emission tomography. Cancer Res, 1998. 58(19): p. 4333-41.

37. Haberkorn, U., Altmann, A., Morr, I., Knopf, K. W., Germann, C., Haeckel, R., Oberdorfer, F., van Kaick, G., Monitoring gene therapy with herpes simplex virus thymidine kinase in hepatoma cells: uptake of specific substrates. J Nucl Med, 1997. 38(2): p. 287-94.

38. Singh, A., Massoud, T. F., Deroose, C., Gambhir, S. S., Molecular imaging of reporter gene expression in prostate cancer: an overview. Semin Nucl Med, 2008. 38(1): p. 9-19.

39. Weissleder, R., Pittet, M. J., Imaging in the era of molecular oncology. Nature, 2008. 452(7187): p. 580-9.

40. Kwon, H.C., Kim, J. H., Kim, K. C., Lee, K. H., Lee, J. H., Lee, B. H., Jang, J. J., Lee, C. T., Lee, H., Kim, C. M., In vivo antitumor effect of herpes simplex virus thymidine kinase gene therapy in rat hepatocellular carcinoma: feasibility of adenovirus-mediated intra-arterial gene delivery. Mol Cells, 2001. 11(2): p. 170-8.

41. Choi, T.H., Ahn, S. H., Kwon, H. C., Choi, C. W., Awh, O. D., Lim, S. M., In vivo comparison of IVDU and IVFRU in HSV1-TK gene expressing tumor bearing rats. Appl Radiat Isot, 2004. 60(1): p. 15-21.

42. Shields, A.F., Grierson, J. R., Kozawa, S. M., Zheng, M., Development of labeled thymidine analogs for imaging tumor proliferation. Nucl Med Biol, 1996. 23(1): p. 17-22.

43. Wu, Y., Fa, M., Tae, E. L., Schultz, P. G., Romesberg, F. E., Enzymatic phosphorylation of unnatural nucleosides. J Am Chem Soc, 2002. 124(49): p. 14626-30.

44. Morin, K.W., Duan, W., Xu, L., Zhou, A., Moharram, S., Knaus, E. E., McEwan, A. J., Wiebe, L. I., Cytotoxicity and cellular uptake of pyrimidine

nucleosides for imaging herpes simplex type-1 thymidine kinase (HSV-1 TK) expression in mammalian cells. Nucl Med Biol, 2004. 31(5): p. 623-30.

45. Hung, S.C., Deng, W. P., Yang, W. K., Liu, R. S., Lee, C. C., Su, T. C., Lin, R. J., Yang, D. M., Chang, C. W., Chen, W. H., Wei, H. J., Gelovani, J. G., Mesenchymal stem cell targeting of microscopic tumors and tumor stroma development monitored by noninvasive in vivo positron emission tomography imaging. Clin Cancer Res, 2005. 11(21): p. 7749-56.

46. Chen, Y.T., Bradley, A., A new positive/negative selectable marker, puDeltatk, for use in embryonic stem cells. Genesis, 2000. 28(1): p. 31-5.

47. Koehne, G., Doubrovin, M., Doubrovina, E., Zanzonico, P., Gallardo, H. F., Ivanova, A., Balatoni, J., Teruya-Feldstein, J., Heller, G., May, C., Ponomarev, V., Ruan, S., Finn, R., Blasberg, R. G., Bornmann, W., Riviere, I., Sadelain, M., O'Reilly, R. J., Larson, S. M., Tjuvajev, J. G., Serial in vivo imaging of the targeted migration of human HSV-TK-transduced antigen-specific lymphocytes. Nat Biotechnol, 2003. 21(4): p. 405-13.

48. Koehne, G., Gallardo, H. F., Sadelain, M., O'Reilly, R. J., Rapid selection of antigen-specific T lymphocytes by retroviral transduction. Blood, 2000. 96(1): p. 109-17.

49. Koehne, G., Smith, K. M., Ferguson, T. L., Williams, R. Y., Heller, G., Pamer, E. G., Dupont, B., O'Reilly, R. J., Quantitation, selection, and functional characterization of Epstein-Barr virus-specific and alloreactive T cells detected by intracellular interferon-gamma production and growth of cytotoxic precursors. Blood, 2002. 99(5): p. 1730-40.

50. Tjernberg, J., Ekdahl, K. N., Lambris, J. D., Korsgren, O., Nilsson, B., Acute antibody-mediated complement activation mediates lysis of pancreatic islets cells and may cause tissue loss in clinical islet transplantation. Transplantation, 2008. 85(8): p. 1193-9.

51. Moberg, L., The role of the innate immunity in islet transplantation.

Ups J Med Sci, 2005. 110(1): p. 17-55.

52. Rood, P.P., Bottino, R., Balamurugan, A. N., Smetanka, C., Ayares, D., Groth, C. G., Murase, N., Cooper, D. K., Trucco, M., Reduction of early graft loss after intraportal porcine islet transplantation in monkeys. Transplantation, 2007. 83(2): p. 202-10.

53. van der Windt, D.J., et al., Rapid loss of intraportally transplanted islets: an overview of pathophysiology and preventive strategies. Xenotransplantation, 2007. 14(4): p. 288-97.

국문요약

분자영상을 위한 방사옥소표지 1-(2′-fluoro-2-deoxy-D-arabinofuranosyl)-5-iodouracil (FIAU)과 1-(2′-fluoro-2-deoxy-D-ribofuranosyl)-5-iodouracil (FIRU)의 비교평가

연세대학교 대학원
임상병리학과
홍 수희

리포터 유전자를 발현을 통한 분자영상분석은 생체 내에서 유전자 발현평가가 가능하다는 큰 장점을 가지고 있다. 이러한 분자영상을 얻기 위해 Herpes Simplex Virus type 1 thymidine kinase (HSV1-TK) 유전자가 리포터 유전자로써 널리 사용되고 있다. Thymidine만을 인산화 하는 mammalian thymidine kinase와 달리 HSV1-TK는 기질 특이성이 약해 purine, pyrimidine nucleoside 뿐만 아니라 그 유도체와도 반응하여 인산화 시키는 특성을 가지고 있다. FIAU와 FIRU는 각각 당의 2′위치에 arabino와 ribo 형태로 fluorine이 결합된 pyrimidine nucleoside 유도체로써 HSV1-TK와의 반응을 통해 세포와 동물 영상에 이용될 수 있다. 본 연구에서는 이 두 물질이 HSV1-TK를 발현하는 세포의 분자영상에서 어떻게 작용하는지 비교분석하고자 하였다.

우선 FIAU와 FIRU를 방사옥소표지 반응 후 HPLC로 정제하여 99% 이상의 방사화학순도로 표지된 FIAU와 FIRU를 얻었다. 세포실험과 동물실험을 위해 MCA 간암세포주와 HSV1-TK를 발현하는 MCA세포를 이용하였다. 이 두 세포주를 이용하여 FIAU와 FIRU의 세포독성과 HSV1-TK 유전자 발현의 연관성을 분석하고자 하였다. MCA-TK 세포에서 FIAU는 ganciclovir(GCV)에 비해 세포독성이 컸고, FIRU는 GCV 보다 독성이 작았다. 방사옥소표지된 이 두 화합물을

MCA와 MCA-TK 세포에 0.5시간, 1시간, 2시간, 4시간동안 반응시켜 세포내 섭취정도를 비교하였다. MCA-TK 세포 내에서는 FIAU와 FIRU 둘 다 4시간까지 섭취량이 증가되는 현상을 보였지만, MCA 세포 내에서는 섭취량이 현저하게 낮았다. FIAU는 30.24 %ID 정도가 섭취되었고, FIRU는 15.02 %ID 정도 섭취되었다.

분자영상을 얻을 수 있는 두 물질의 활성을 비교하기 위해 MCA 세포와 MCA-TK 세포를 면역결핍 누드마우스의 양쪽 어깨에 각각 이식하여 동물모델을 준비하여, 동위원소가 표지된 FIAU와 FIRU를 이식된 종양을 가지고 있는 마우스에 정맥 투여 후 microPET과 γ-camera으로 분자영상을 얻었다. FIAU를 투여하였을 때 288 시간 이상 γ-camera를 이용한 MCA-TK 종양영상을 선명하게 확인할 수 있었으나 MCA 종양영상은 수 시간 후에 관찰이 불가능 하였다. MCA-TK와 MCA 종양 영상의 %ID/g 비가 FIRU의 경우는 약 1.2배인 것에 비해 FIAU는 187.3배를 보였다. 세포추적 영상평가에서 폐로 이동한 를 섭취한 세포를 72시간까지 관찰할 수 있었다. 그러나 종양전이모델에서는 방사옥소 표지된 FIAU의 투여를 통해 전이암의 영상을 얻을 수 없었다.

이상의 결과로써, HSV1-TK 유전자 발현을 통한 분자영상을 얻는 데에 FIAU가 FIRU에 비해 보다 효율적인 기질로 작용한다는 것을 알 수 있었다. 또한 FIAU를 이용하여 줄기세포나 면역세포를 생체 내에서 장기간 추적하는 데 유용할 것으로 보인다.

핵심어: 리포터 유전자, HSV1-TK, FIAU, FIRU, PET, γ-camera

감사의 글

대학원에 입학하여 지나온 시간들은 제 인생에서 커다란 배움이 되었던 시간이었습니다. 2년 반이란 시간은 아쉬움과 부족함이 많았지만 나도 무언가 할 수 있다는 자신감과 앞으로 나아가야 할 길에 대한 생각을 가지게 끔 해준 시간이었습니다. 이렇게 많은 배움을 주신 많은 분들께 깊이 감사의 말씀을 올립니다. 저를 도와주신 분들이 이렇게 많음에도 일일이 찾아뵙지 못하고 글로 감사드리는 점이 죄송할 따름입니다.

우선 논문이 나오기 까지 많은 배려와 지도를 해주신 박용석 교수님과 최태현 박사님 정말 감사드립니다. 논문심사 과정을 통해 아낌없는 격려와 지도를 해주신 김종배 교수님과 오옥두 교수님께 진심으로 감사드립니다. 그리고 많은 가르침을 주신 김태우 교수님, 양용석 교수님, 이혜영 교수님, 김윤석 교수님께도 감사드립니다.

석사 학기를 시작하면서 마칠 때 까지 많은 도움을 주신 한국원자력의학원 분자영상연구부 임상무 과장님, 최창운 과장님, 천기정 과장님, 김병일 과장님, 강주현 박사님, 김경민 박사님, 김광일 선생님, 김정영 박사님, 김종국 박사님, 김진수 선생님, 문병석 선생님, 문철 박사님, 박현 선생님, 안광일 박사님, 안순혁 선생님, 오동현 선생님, 이교철 박사님, 이태섭 박사님, 우광선 선생님, 우상근 박사님, 전권수 박사님, 정수영 선생님, 정위섭 선생님, 홍명찬 선생님, 현석오빠, 재호오빠, 수진씨, 진주씨, 주희씨, 재준씨, 상진씨, 치훈씨, 선임씨, 정향씨, 대덕씨, 영범씨, 재용씨 모두 감사드립니다.

그리고 함께 하였기에 다행이고 행복이었던 은댕언니 정말 고맙고, 지금은 함께 없지만 거의 2년의 함께 했던 은아언니, 종찬오빠에게도 고마운 마음을 전합니다.

학교에 가면 늘 환하게 반겨주던 우리 세포생물학 연구실사람들! 귀염둥이 연경언니, 늘 바빠보였던 정석오빠, 깜찍한 진이, 엉뚱쟁이 화연이, 이미 졸업했지만 늘 유쾌해서 기억에 남는 경혜언니, 든든한 인호오빠, 그리고 친절하신 근식선배님 정말 고맙습니다. 그리고 형엽오빠, 도완오빠, 인수오빠, 규상오빠, 은아언니, 은주언

니, 관훈오빠, 방혜은선생님, 현철선배님, 현우오빠, 연임언니, 상정이, 그리고 새로 대학원의 문을 열고 들어온 지용이, 김소진선생님, 최동혁, 김성현, 먼저 졸업한 혜은, 정례에게도 고마운 마음을 전합니다.

또 점점 여성스러워지시는 수인언니와 오실 때 마다 아낌없는 조언을 주시는 남상민 선배님, 지금은 다른 곳으로 가신 진현석 선배님 정말 감사합니다.

그리고 대학에 입학하면서부터 지금까지 7년이나 늘 함께 지내는 고맙고 소중한 친구 세나, 은미, 현주 너희들 덕분에 지금이 있는 것 같아서 정말 고맙고, 여고 시절의 추억을 아직까지 함께 나눌 수 있는 따뜻한 친구 목경, 화숙, 하나에게도 고맙다고 전하고 싶습니다.

손녀 딸 공부한다고 좋아하셨던 할머니, 아파도 손녀딸 놀랄까봐 내색도 잘 안하셔서 괜히 죄송하고, 지금까지 함께 있기에 정말 감사드립니다. 또 같이 생활했던 은실고모, 고모부, 덕기, 지혜 건강하게 지냈으면 좋겠고 같이 생활하면서 이런저런 일이 있었지만 그저 고마운 마음만 듭니다. 큰고모, 고모부, 둘째고모, 둘째고모부, 큰아버지, 큰어머니, 작은아버지, 작은어머니, 막내작은아버지, 막내작은어머니, 그리고 사촌들 정말 고맙습니다. 그리고 사랑합니다.

마지막으로 사랑하는 엄마, 아빠! 딸이 공부 더 한다고 했을 때 무조건적으로 믿고 지지해주셔서 감사합니다. 나의 동생 동원! 누나 때문에 늘 힘들었을 텐데 내색도 안하고 고맙다.

앞으로 함께 할 수많은 시간이 모두에게, 그리고 모두와 함께 행복으로 다가왔으면 좋겠습니다.